

This article was downloaded by:

On: 25 January 2011

Access details: *Access Details: Free Access*

Publisher *Taylor & Francis*

Informa Ltd Registered in England and Wales Registered Number: 1072954 Registered office: Mortimer House, 37-41 Mortimer Street, London W1T 3JH, UK



Separation Science and Technology

Publication details, including instructions for authors and subscription information:

<http://www.informaworld.com/smpp/title~content=t713708471>

Theory of Clarifier Operation. III. Sludge Blanket and Upflow Reactor-Clarifiers

Ann N. Clarke^a; David J. Wilson^a; James H. Clarke^b

^a DEPARTMENTS OF CHEMISTRY AND ENVIRONMENTAL ENGINEERING, VANDERBILT UNIVERSITY, NASHVILLE, TENNESSEE ^b ASSOCIATED WATER AND AIR RESOURCES ENGINEERS, INC., NASHVILLE, TENNESSEE

To cite this Article Clarke, Ann N. , Wilson, David J. and Clarke, James H.(1978) 'Theory of Clarifier Operation. III. Sludge Blanket and Upflow Reactor-Clarifiers', *Separation Science and Technology*, 13: 10, 895 — 915

To link to this Article: DOI: 10.1080/01496397808057137

URL: <http://dx.doi.org/10.1080/01496397808057137>

PLEASE SCROLL DOWN FOR ARTICLE

Full terms and conditions of use: <http://www.informaworld.com/terms-and-conditions-of-access.pdf>

This article may be used for research, teaching and private study purposes. Any substantial or systematic reproduction, re-distribution, re-selling, loan or sub-licensing, systematic supply or distribution in any form to anyone is expressly forbidden.

The publisher does not give any warranty express or implied or make any representation that the contents will be complete or accurate or up to date. The accuracy of any instructions, formulae and drug doses should be independently verified with primary sources. The publisher shall not be liable for any loss, actions, claims, proceedings, demand or costs or damages whatsoever or howsoever caused arising directly or indirectly in connection with or arising out of the use of this material.

Theory of Clarifier Operation. III. Sludge Blanket and Upflow Reactor-Clarifiers

ANN N. CLARKE and DAVID J. WILSON*

DEPARTMENTS OF CHEMISTRY AND ENVIRONMENTAL ENGINEERING
VANDERBILT UNIVERSITY
NASHVILLE, TENNESSEE 37235

JAMES H. CLARKE

ASSOCIATED WATER AND AIR RESOURCES ENGINEERS, INC.
NASHVILLE, TENNESSEE 37204

Abstract

The operation of three designs of axially symmetric continuous-flow upflow clarifiers is modeled by means of the continuity equations. Class III operation (hindered settling) with flocculating slurries is considered, and the larger particles are permitted to disintegrate under the influence of viscous drag forces by a first-order process. The equations are integrated numerically, and the dependence of clarifier performance on clarifier type and hydraulic loadings is explored. A number of applications to clarifier design are suggested.

INTRODUCTION

Ives in 1968 published an analysis of a conical sludge blanket clarifier in steady-state operation (1). In these clarifiers, shaped like an inverted cone with the tip cut off, slurry is received at the bottom and rises through the clarifier at an ever-decreasing speed; where the rate of rise of the liquid has been reduced to the rate of fall of a slurry particle relative to the liquid, a sludge blanket is formed. Sludge is continuously wasted from this layer, and clarified effluent is discharged at the top. Ives also took ortho-

*To whom reprint requests should be addressed.

kinetic flocculation into account, although in only a qualitative way. His analysis resulted in the development of some remarkably simple design formulas, use of which he illustrated.

In 1972, Chang (2) presented in his Ph.D. thesis a very elegant treatment of settling in quiescent and upflow clarifiers, and a comprehensive review of the literature. To our knowledge this fine work was not published elsewhere, and the complexity of the computer program simulating clarifier operation and the size and speed of computer which appears to be needed make this approach inaccessible to many engineers.

In earlier papers in this series we have modeled quiescent hindered settling with flocculating slurries (3) and hindered settling of flocculating particles in rectangular clarifiers (4) by numerical integration of the continuity equations with suitable boundary conditions. In the first of these papers we reviewed the literature on hindered settling. Here we extend the basic approach used in the first paper for the analysis of upflow sludge blanket clarifiers in which the feed is at the bottom and sludge is wasted part way up the clarifier; we then turn to clarifiers in which the influent is fed part way up the clarifier and sludge is wasted from the bottom.

ANALYSIS, UPFLOW SLUDGE BLANKET CLARIFIERS

We take the continuity equations for coalescing and disintegrating floc particles in an axially symmetric sludge blanket clarifier to be

$$\begin{aligned} \frac{\delta c_n}{\delta t}(x, t) = & \frac{-1}{A(x)} \frac{\partial}{\partial x} (A v'_n c_n) + \frac{1}{A} \frac{\partial}{\partial x} \left(A D \frac{\delta c_n}{\delta x} \right) \\ & + \sum_{j=1}^{[n/2]} \{c_n c_{n-j} |v_j - v_{n-j}| \pi (r_j + r_{n-j})^2 - k_{j,n-j}^n c_n\} \\ & - \sum_{j=1}^{N-n} c_n c_j |v_n - v_j| \pi (r_n + r_j)^2 + \sum_{j=n+1}^n k_{n,j-n}^j c_j (1 + \delta_{j,2n}) \quad (1) \end{aligned}$$

Notation is as follows:

x = distance from bottom of clarifier

l = position of sludge blanket waste plane

L = position of top of clarifier

$A(x)$ = cross-sectional area of clarifier at x , $= \pi \left[r_e + \frac{x}{L} (r_u - r_e) \right]^2$

r_e = radius of the bottom of the clarifier

r_u = radius of the top of the clarifier

Q_{waste} = volume flow rate of sludge wastage

Q_{feed} = volume flow rate of influent feed

$c_n(x, t)$ = number of n -particles per unit volume at x and t

V_1 = volume of an elementary particle

V_k = volume of a k -particle = kV_1

r_k = radius of a k -particle, assumed spherical,

$$= \left(\frac{3kV_1}{4\pi} \right)^{1/3}, \quad k = 1, 2, 3, \dots$$

$v_k = -u_k$

$$u_k = \frac{2[\Delta\rho(c)]gr_k^2}{9\eta(c) \left\{ 1 + \frac{1}{4} \left(\frac{\rho_{sl}r_ku_k}{2\eta} \right)^{1/2} + 0.34\rho_{sl}r_ku_k \right\}}$$

= |velocity| of a k -particle relative to the surrounding slurry (2)

$$\eta = \eta_0 \exp \left[\frac{2.5C + 2.7C^2}{1 - 0.609C} \right]$$

= viscosity of slurry having solids volume fraction C (3)

η_0 = viscosity of liquid

$$C = \sum_{n=1}^N c_n V_n = \text{solids volume fraction at } x, t$$

$\rho_{sl} = \rho_s C + \rho_l(1 - C)$ = slurry density

$\Delta\rho = (\rho_s - \rho_l)(1 - C)$ = difference in density between a solid particle and the surrounding slurry

ρ_s = density of solid

ρ_l = density of liquid

D = axial diffusion constant

g = gravitational constant

v'_k = velocity of k -particle relative to the laboratory

v'' = velocity of the liquid relative to the laboratory

$k_{n,m-n}^m$ = rate constant for the disruption of an m -particle into an n -particle and an $(m - n)$ -particle

$\delta_{n,j} = 1$ if $n = j$, = 0 if $n \neq j$

N = number of 1-particles in largest permitted particle

$[N/2]$ = greatest integer $\leq N/2$

We need to calculate the laboratory velocities v'_k of the falling particles; this is done as follows. Generally we have

$$v'_k = v'' + v_k \quad (4)$$

where v_k is calculated (for low to intermediate Reynolds numbers) from Eq. (2). Below the sludge waste plane ($0 < x < l$) we have

$$Q_{\text{feed}} = Q_f(t) = A(x)\{[1 - C(x, t)]v''(x, t) + \sum_{n=1}^N c_n(x, t)V_n v'_n(x, t)\} \quad (5)$$

which yields, on use of Eq. (4),

$$v'' = \frac{Q_f}{A} - \sum_{n=1}^N c_n V_n v_n \quad (6)$$

and

$$v'_k = \frac{Q_f}{A} + v_k - \sum_{n=1}^N c_n V_n v_n \quad (7)$$

In similar fashion, above the sludge waste plane ($l < x < L$) we have

$$v'_k(x, t) = \frac{Q'_f}{A(x)} + v_k - \sum_{n=1}^N c_n V_n v_n \quad (8)$$

where $Q'_f = Q_{\text{feed}} - Q_{\text{waste}}$.

Inasmuch as Eqs. (1) constitute a highly nonlinear set of coupled second-order partial differential equations, we immediately resign ourselves to the necessity of developing a discrete representation of Eqs. (1) which yields a system of first-order differential equations with t as the independent variable. We partition the clarifier into a set of horizontal slabs of thickness Δx , as indicated in Fig. 1, and then carry out a mass balance on each slab for each type of particle, making sure that in doing so we conserve particles at each boundary between slabs. We let

$$\begin{aligned} A(p) &= A[p - 1/2]\Delta x, \text{ cross-sectional area of clarifier at } x = \\ &(p - 1/2)\Delta x \\ &= \pi \left[r_e + (r_u - r_e) \frac{p - 1/2}{I} \right]^2 \text{ for our model} \end{aligned}$$

$$c(n, p, t) = c_n[(p - 1/2)\Delta x, t]$$

$$\mathbf{c}(p, t) = (c_1, c_2, \dots, c_N)$$

$c^0(n, t)$ = concentration of n -particles in the influent

$$v(n, p, t) = v_n[(p - 1/2)\Delta x, t]$$

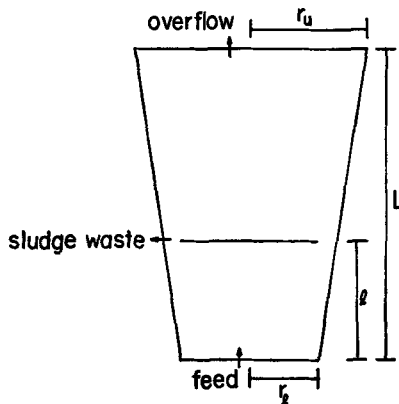


FIG. 1. Sludge blanket clarifier.

$$v'(n, p, t) = v'_n[(p - 1/2)\Delta x, t]$$

$$\begin{aligned} S(u) &= 0, \text{ if } u < 0 \\ &= 1, \text{ if } u \geq 0 \end{aligned}$$

$\text{Floc}[n, c(p, t)]$ = the three sums in Eq. (1) evaluated at the point $(p - 1/2)\Delta x$ and at time t

m = index of the compartment containing the sludge waste plane

I = index of the top compartment

$$k_{j,n-j}^n = \frac{\kappa n n!}{j!(n-j)!} \cdot \frac{[N/2]!(j - [N/2])!}{N N!} \quad (9)$$

At a general point ($i \neq 1, m, I$), we represent Eq. (1) as follows. (We drop the axial dispersion term for simplicity and for lack of a good estimate of the axial diffusion constant D .)

$$\begin{aligned} \frac{\partial c}{\partial t}(n, i, t) &= \frac{1}{A(i)\Delta x} \{ v'(n, i - 1, t)c(n, i - 1, t)A(i - 1)S[v'(n, i - 1, t)] \\ &\quad + v'(n, i, t)c(n, i, t)A(i)(S[-v'(n, i, t)] - S[v'(n, i, t)]) \\ &\quad - v'(n, i + 1, t)c(n, i + 1, t)A(i + 1)S[-v'(n, i + 1, t)] \} \\ &\quad + \text{Floc}[n, c(i, t)] \end{aligned} \quad (10)$$

If $i \leq m - 1$, calculate v' from Eq. (7); if $i \geq m + 1$, calculate v' from Eq. (8).

At the sludge wasting plane, we have

$$\begin{aligned}
 \frac{\partial c}{\partial t}(n, m, t) = & \frac{1}{A(m)\Delta x} \{ v'_L(n, m-1, t)c(n, m-1, t)A(m-1) \\
 & \times S[v'_L(n, m-1, t)] \\
 & + v'_L(n, m, t)c(n, m, t)A(m)S[-v'_L(n, m, t)] \\
 & - v'_u(n, m, t)c(n, m, t)A(m)S[v'_u(n, m, t)] \\
 & - v'_u(n, m+1, t)c(n, m+1, t)A(m+1) \\
 & \times S[-v'_u(n, m+1, t)] \} \\
 & + \text{Floc}[n, \mathbf{c}(m, t)] - \frac{Q_{\text{waste}}}{A(m)\Delta x} c(n, m, t) \quad (11)
 \end{aligned}$$

Here the v'_L are calculated from Eq. (7) and the v'_u from Eq. (8).

At the bottom of the clarifier mass balance yields

$$\begin{aligned}
 \frac{\partial c}{\partial t}(n, 1, t) = & \frac{1}{A(1)\Delta x} \{ v'(n, 1, t)c(n, 1, t)A(1) \\
 & \times |S[-v'(n, 1, t)] - S[v'(n, 1, t)]| \\
 & - v'(n, 2, t)c(n, 2, t)A(2)S[-v'(n, 2, t)] \} \\
 & + \text{Floc}[n, \mathbf{c}(1, t)] + \frac{Q_{\text{feed}}c^\circ(n, t)}{A(1)\Delta x} \quad (12)
 \end{aligned}$$

And at the top of the clarifier,

$$\begin{aligned}
 \frac{\partial c}{\partial t}(n, I, t) = & \frac{1}{A(I)\Delta x} \{ v'(n, I, t)c(n, I, t)A(I) \\
 & \times |S[-v'(n, I, t)] - S[v'(n, I, t)]| \\
 & + v'(n, I-1, t)c(n, I-1, t)A(I-1)S[v'(n, I-1, t)] \} \\
 & + \text{Floc}[n, \mathbf{c}(I, t)] \quad (13)
 \end{aligned}$$

We can now write Eqs. (10)–(13) in abbreviated notation as

$$\frac{dc}{dt}(n, i, t) = f[n, i, \mathbf{c}(t)] \quad (14)$$

where $\mathbf{c}(t)$ represents $c(1, 1, t), \dots, c(N, I, t)$. We then use a simple predictor-corrector method for integrating this system of equations. We start as follows:

predictor

$$c^*(n, i, \Delta t) = c(n, i, 0) + \Delta t \{f[n, i, \mathbf{c}(0)]\} \quad (15)$$

corrector

$$c(n, i, \Delta t) = c(n, i, 0) + \frac{\Delta t}{2} \{f[n, i, \mathbf{c}(0)] + f[n, i, \mathbf{c}^*(\Delta t)]\} \quad (16)$$

After the integration is started, one can use the following somewhat improved algorithm:

predictor

$$c^*(n, i, t + \Delta t) = c(n, i, t - \Delta t) + 2\Delta t \{f[n, i, \mathbf{c}(t)]\} \quad (17)$$

corrector

$$c(n, i, t + \Delta t) = c(n, i, t) + \frac{\Delta t}{2} \{f[n, i, \mathbf{c}(t)] + f[n, i, \mathbf{c}^*(t + \Delta t)]\} \quad (18)$$

Use of the computer program which solves this system generates vast quantities of data which the computer must summarize if one is to avoid being overwhelmed with output. We summarize the results as follows.

First, from time to time during the integration we print out clarifier profiles of the solids volume fraction, given by

$$\text{SVF}(i, t) = \sum_n c(n, i, t) V_n \quad (19)$$

Second, we calculate the influent solids volume fraction (ISVF), the sludge solids volume fraction (SSVF), and the effluent solids volume fraction (ESVF), given by

$$\text{ISVF} = \sum_{n=1}^N c^0(n, t) V_n \quad (20)$$

$$\text{SSVF} = \sum_{n=1}^N c(n, m, t) V_n [v'_L(n, m, t) - v'_n(n, m, t) A_{(m)} / Q_{\text{waste}}} \quad (21)$$

$$\text{ESVF} = \sum_{n=1}^N c(n, I, t) V_n v'_u(n, m, t) S[v'_u(n, m, t)] A_{(I)} / (Q_{\text{feed}} - Q_{\text{waste}}) \quad (22)$$

The influent solids flux (ISF), sludge solids flux (SSF), and effluent solids flux (ESF) are given by

$$\text{ISF} = \text{ISVF} \cdot Q_{\text{feed}} \quad (23)$$

$$SSF = SSVF \cdot Q_{waste} \quad (24)$$

$$ESF = ESVF \cdot (Q_{feed} - Q_{waste}) \quad (25)$$

Lastly, the percent removal of solids in the sludge is given by

$$\% \text{ removal} = R = \frac{100SSF}{ISF} \quad (26)$$

ANALYSIS, UPFLOW REACTOR-CLARIFIERS

We examine the operation of upflow reactor-clarifiers of the type diagrammed in Fig. 2. Here reaction to form the floc takes place in the inner conical section, in which the liquid may be mixed; it is then discharged in a relatively quiescent state from the bottom of this inner cone into the cylindrical clarifier section. Here the bulk of the liquid rises to the top and is discharged as clarifier overflow; a smaller fraction sinks to the bottom with the solids and is discharged as sludge.

We use the same notation as before, except as indicated below:

m = index of slab containing the influent feed plane

r_c = radius of outer (cylindrical) shell of clarifier

r_{bot} = radius of the bottom of the conical section

r_{top} = radius of the top of the conical section

A_i = cross-sectional area of the clarifier section at the middle of the i th slab

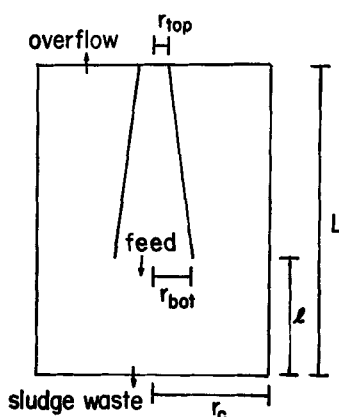


FIG. 2. Upflow reactor-clarifier.

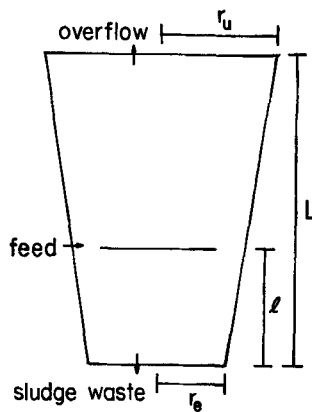


FIG. 3. Another design of upflow clarifier.

$$= \pi \left\{ r_c^2 - S(i-m) \left[r_{\text{bot}} - (r_{\text{bot}} - r_{\text{top}}) \frac{i-m}{I-m} \right]^2 \right\} \quad (27)$$

Our general discrete approximation to Eq. (1) is

$$\begin{aligned} \frac{\partial c}{\partial t}(n, i, t) = & \frac{1}{A(i)\Delta x} \{ v'(n, i-1, t) c(n, i-1, t) A(i-1) S[v'(n, i-1, t)] \\ & + v'(n, i, t) c(n, i, t) A(i) |S[-v'(n, i, t)] - S[v'(n, i, t)]| \\ & - v'(n, i+1, t) c(n, i+1, t) A(i+1) S[-v'(n, i+1, t)] \} \\ & + \text{Floc}[n, \mathbf{c}(i, t)] \end{aligned} \quad (28)$$

At the bottom of the clarifier

$$\begin{aligned} \frac{\partial c}{\partial t}(n, 1, t) = & \frac{1}{A(1)\Delta x} \{ v'(n, 1, t) c(n, 1, t) A(1) |S[-v'(n, 1, t) - S[v'(n, 1, t)]| \\ & - v'(n, 2, t) c(n, 2, t) A(2) S[-v'(n, 2, t)] \} \\ & + \text{Floc}[n, \mathbf{c}(1, t)] \end{aligned} \quad (29)$$

At the top of the clarifier we have

$$\begin{aligned} \frac{\partial c}{\partial t}(n, I, t) = & \frac{1}{A(I)\Delta x} \{ v'(n, I-1, t) c(n, I-1, t) A(I-1) S[v'(n, I-1, t)] \\ & + v'(n, I, t) c(n, I, t) A(I) |S[-v'(n, I, t)] - S[v'(n, I, t)]| \} \\ & + \text{Floc}[n, \mathbf{c}(I, t)] \end{aligned} \quad (30)$$

At the feed plane

$$\begin{aligned}
 \frac{\partial c}{\partial t}(n, m, t) = & \frac{1}{A(m)\Delta x} \{ v'_L(n, m - 1, t)c(n, m - 1, t)A(m - 1) \\
 & \times S[v'_L(n, m - 1, t)] \\
 & + v'_L(n, m, t)c(n, m, t)A(m)S[-v'_L(n, m, t)] \\
 & - v'_u(n, m, t)c(n, m, t)A(m)S[v'_u(n, m, t)] \\
 & - v'_u(n, m + 1, t)c(n, m + 1, t)A(m + 1)S[-v'_u(n, m + 1, t)] \} \\
 & + \text{Floc}[n, \mathbf{c}(m, t)] + \frac{Q_{\text{feed}}c^\circ(n, t)}{A(m)\Delta x} \quad (31)
 \end{aligned}$$

Next we need to calculate the velocities of the floc particles with respect to the lab in the regions above and below the feed plane. Below the feed plane we have

$$v'_L(n, i, t) = v(n, i, t) - A_i^{-1}Q_{\text{waste}} - \sum_{k=1}^N v(k, i, t)c(k, i, t)V_k \quad (32)$$

Above the feed plane we have

$$v'_u(n, i, t) = v(n, i, t) + A_i^{-1}(Q_{\text{feed}} - Q_{\text{waste}}) - \sum_{k=1}^N v(k, i, t)c(k, i, t)V_k \quad (33)$$

We use Eq. (32) in Eqs. (31), (29), and (28) if $i < m$; we use Eq. (33) in Eqs. (31), (30), and (28) if $i > m$.

Again we are plagued by an overwhelming quantity of data available from the computer, which we summarize as follows. We obtain the clarifier profile of solids volume fraction from Eq. (19) as before. The influent solids volume fraction is given by Eq. (20) as before, the effluent solids volume fraction is given by Eq. (22), and the sludge solids volume fraction is given by

$$\text{SSVF} = \sum_{n=1}^N c(n, 1, t)V_n v'(n, 1, t)A_1/Q_{\text{waste}} \quad (34)$$

Influent solids flux, sludge solids flux, effluent solids flux, and percent removal of solids in the sludge are given by Eqs. (23)–(26), as before.

RESULTS, SLUDGE BLANKET CLARIFIERS

To illustrate an application of our clarifier simulator, we exhibit in Figs. 4–9 the dependence of sludge blanket clarifier operation on feed

rate; see Fig. 1. These figures exhibit the variation with time of the solids volume fraction at various points within the clarifier for feed rates of 2500, 3000, 3500, 4000, and 4500 ml/sec. The values of the parameters used are given in the caption of Fig. 4.

In Fig. 4 the feed rate of 2500 ml/sec is well below the capacity of the clarifier for this influent. The top of the principal sludge blanket is gradually rising to the sludge wasting plane, and a sparse secondary blanket of single particles is slowly developing in level fifteen. The percent solids removal is 100% as measured by effluent solids volume fraction (ESVF); it is 83.18% and rising after 300 sec as measured by sludge solids volume fraction (SSVF).

In Fig. 5 the feed rate has been increased to 3000 ml/sec. By 800 sec the principal sludge blanket is well established, and we see a secondary accumulation layer at the top of the clarifier. By 3000 sec the principal sludge blanket has moved up to the ninth level in the clarifier, and the secondary blanket has developed at level twelve. The percent solids removal after 3000 sec is 88.85% (as measured by SSVF) and still increasing; it is 99.43% (as measured by ESVF) and slightly decreasing. The system is approaching, but has not yet quite reached, steady-state operation.

The feed rate is 3500 ml/sec in Fig. 6. The principal sludge blanket is established more quickly than at the lower feed rates, and is less dense.

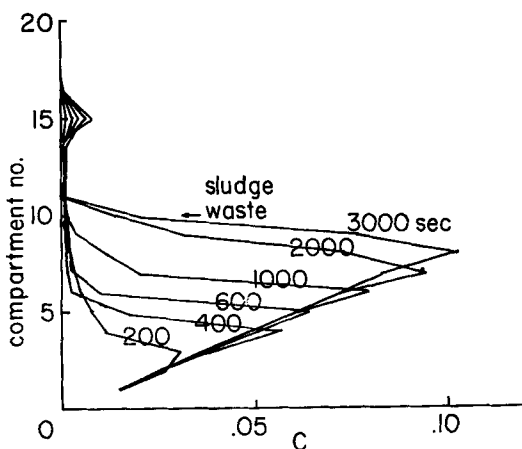


FIG. 4. Sludge blanket clarifier solids distribution, $\eta_0 = 0.01 P$, $\rho_s = 1.05 \text{ g/ml}$, $\rho_i = 1.00 \text{ g/ml}$, $r_1 = 0.02 \text{ cm}$, $l = 47.5 \text{ cm}$, $L = 100 \text{ cm}$, $r_t = 30 \text{ cm}$, $r_u = 50 \text{ cm}$, $\kappa = 0.01 \text{ sec}^{-1}$, $Q_{\text{waste}} = 200 \text{ cm}^3/\text{sec}$, $I = 20$, $N = 4$, $c^o(n, t) = \text{const}/n^2$, $Q_{\text{feed}} = 2500 \text{ ml/sec}$, influent solids volume fraction (ISVF) = 0.002, % removals = 83.18% (SSVF) and 100.00% (ESVF).

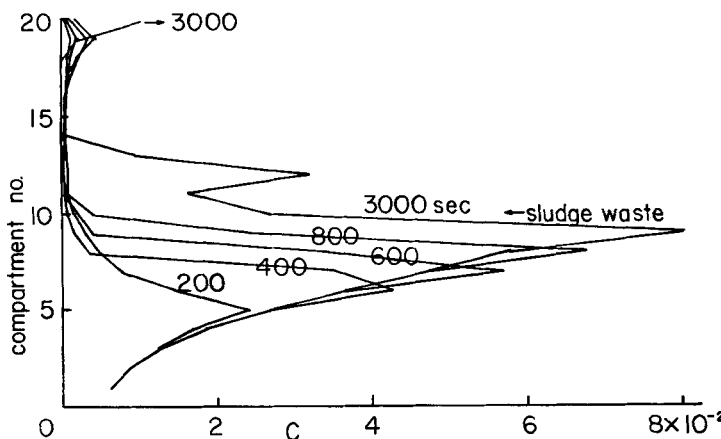


FIG. 5. Sludge blanket clarifier solids distribution. $Q_{\text{feed}} = 3000 \text{ ml/sec}$, % removals at 3000 sec = 88.85% and rising (SSVF), 99.43% (ESVF).

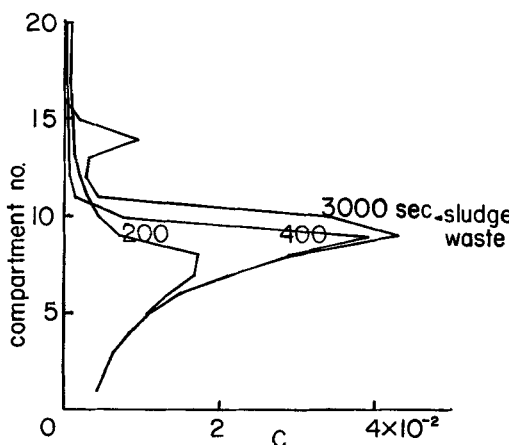


FIG. 6. Sludge blanket clarifier solids distribution. $Q_{\text{feed}} = 3500 \text{ ml/sec}$, % removals at 3000 sec = 97.82% (SSVF), 99.84% (ESVF).

The increased flow rate prevents the accumulation of single particles at the top of the clarifier, and the other secondary blanket has been pushed up from level twelve to level fourteen. Removal efficiency is still high; after 3000 sec it is 97.82% (by SSVF) or 99.84% (ESVF).

We have increased the feed rate to 4000 ml/sec in Fig. 7. At this feed rate the principal sludge blanket lies well above the sludge waste plane

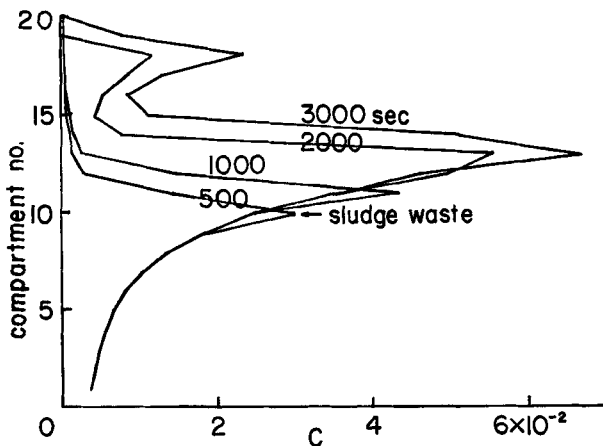


FIG. 7. Sludge blanket clarifier solids distribution. $Q_{\text{feed}} = 4000 \text{ ml/sec}$, % removals at 3000 sec = 61.75% (SSVF), 99.93% and falling (ESVF).

(level ten), and solids are still building up in the upper levels of the clarifier after 3000 sec. The secondary blanket has been pushed to the eighteenth level of the clarifier. There has been a drastic drop in solids removal as the feed rate has increased from 3500 to 4000 ml/sec; the percent solids removal is 61.75% (by SSVF). (The figure of 99.93% calculated from ESVF is obviously unrealistic, given the way in which the secondary blanket is building up in the top of the clarifier.) The clarifier is obviously seriously overloaded hydraulically by this 14% increase in feed rate.

The effects of further hydraulic overloading are shown in Fig. 8; here the feed rate is 4500 ml/sec. The feed rate is now sufficiently high that no secondary blankets form and the principal sludge blanket is evidently being slowly forced out the top of the clarifier. The percent removal (by SSVF) is now only 28.17%; by ESVF it is 52.49% and dropping at 3000 sec.

The sharp drop-off in clarifier efficiency with increasing feed rate is illustrated in Fig. 9, in which SSVF and ESVF removal efficiencies at 3000 sec are plotted against feed rate. Clarifiers of this design apparently exhibit very high efficiencies so long as they are not overloaded, but their performance deteriorates drastically on relatively slight overloading. Inspection of Figs. 4-8 indicates that performance slumps when the concentration maximum of the principal sludge blanket rises above the level from which sludge is wasted. The section of the clarifier above the sludge

wasting level functions only as a buffer; it could help absorb short-term overloads, but it does not appear to increase the steady-state capacity of the clarifier significantly. In particular, the plots in Fig. 8 do not indicate the occurrence of significant fallout of coagulated particles from the rather dense sludge blanket which is formed near the top of the clarifier.

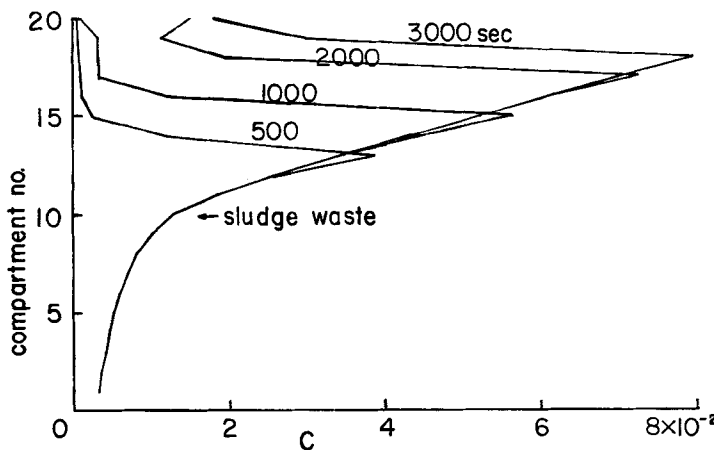


FIG. 8. Sludge blanket clarifier solids distribution. $Q_{\text{feed}} = 4500 \text{ ml/sec}$, % removals at 3000 sec = 28.17% (SSVF), 52.49% and falling (ESVF).

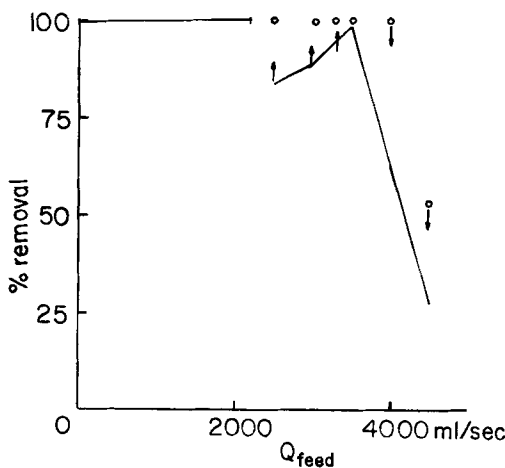


FIG. 9. Sludge blanket clarifier solids removals as functions of feed rate Q_{feed} : \circ , calculated from ESVF; \bullet , calculated from SSVF; \uparrow , increasing at 3000 sec; \downarrow , decreasing at 3000 sec.

RESULTS, REACTOR-CLARIFIERS

We next turn to the effects of feed rate on the operation of reactor-clarifiers of the type illustrated in Fig. 2; these are shown in Figs. 10-15. The influent characteristics and clarifier parameters for all these runs are given in the legend to Fig. 10.

At a feed rate of 1000 ml/sec this clarifier achieves 100% removal, and a steady-state is closely approached after 600 sec. No solids rise above the feed plane (level 10), as shown in Fig. 10. At a feed rate of 1500 ml/sec, shown in Fig. 11, percent removal is 87.99% (SSVF) or 90.30% (ESVF) after 600 sec, by which time the clarifier has essentially reached a steady-state. [On a per unit area basis, this corresponds to a feed rate of 4167 ml/sec for our sludge blanket clarifier; r_{top}^2 (sludge blanket)/ r_c^2 (reactor-clarifier) = 2.778.]

In Fig. 12 we have increased the feed rate to 2000 ml/sec, and the percent removal has dropped to 82.18% (SSVF) or 84.97% (ESVF). This corresponds to a feed rate of 5556 ml/sec in the sludge blanket clarifier. In Fig. 13 the feed rate is 2500 ml/sec; the percent removal is 65.52% (SSVF) or 75.16% (ESVF). Here we see for the first time the formation of a primary sludge blanket. The upper section of the clarifier has not reached a steady-state after 600 sec, and the two percent removal figures

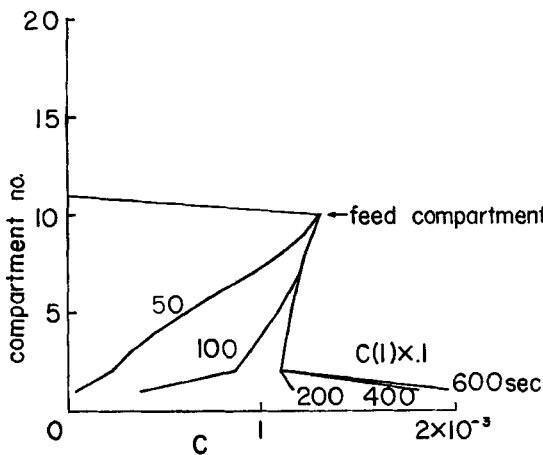


FIG. 10. Reactor-clarifier solids distribution. $L = 100$ cm, $l = 47.5$ cm, $r_{bot} = 10$ cm, $r_{top} = 5$ cm, $r_c = 30$ cm, $Q_{feed} = 1000$ ml/sec, $Q_{waste} = 100$ ml/sec; other parameters as in Fig. 4. Percent removals after 600 sec = 97.5% and rising (SSVF), 100.00% (ESVF).

are still drifting toward each other. The hydraulic loading corresponds to 6944 ml/sec in the sludge blanket clarifier.

In Fig. 14 the feed rate is 3000 ml/sec, and a steady-state is achieved in less than 600 sec. Percent removal figures are 54.24% (SSVF) and 55.50%

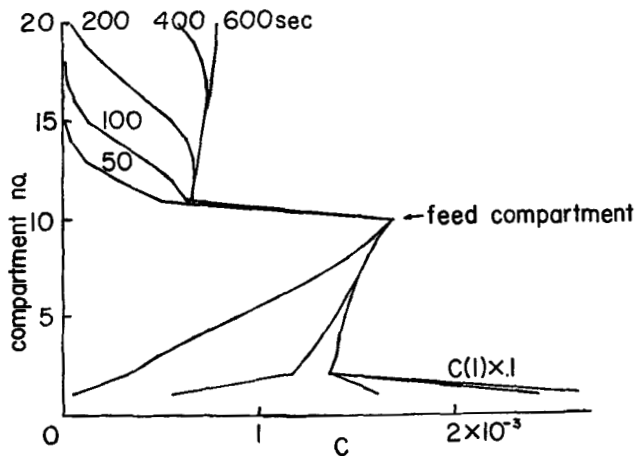


FIG. 11. Reactor-clarifier solids distribution. $Q_{\text{feed}} = 1500 \text{ ml/sec}$; other parameters as in Fig. 10. Percent removal at 600 sec = 87.99% (SSVF) and rising, 90.30% and falling (ESVF).

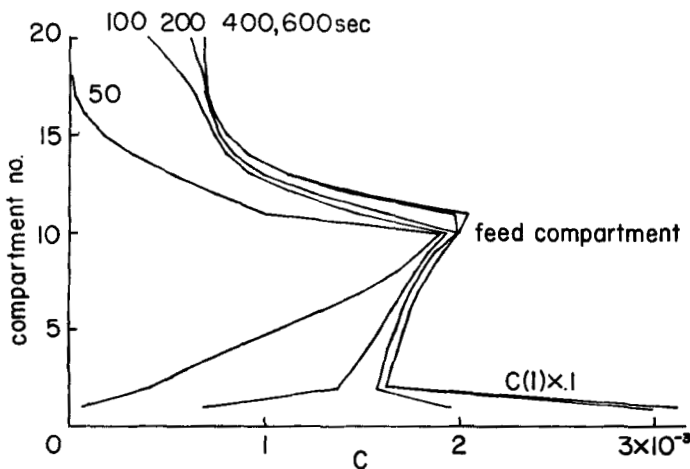


FIG. 12. Reactor-clarifier solids distribution. $Q_{\text{feed}} = 2000 \text{ ml/sec}$, % removal at 600 sec = 82.18% (SSVF), 84.97% (ESVF).

(ESVF), indicating removal of better than half the solids at a flow rate corresponding to 8333 ml/sec for the sludge blanket clarifier.

The behavior of this design of clarifier under overloads is shown in Fig. 15. We see that clarifier efficiency decreases much more slowly as we go past the breakthrough point than it does for the sludge blanket clarifier.

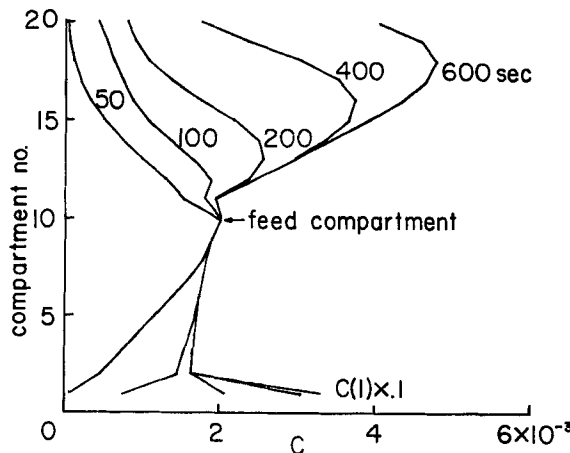


FIG. 13. Reactor-clarifier solids distribution. $Q_{\text{feed}} = 2500 \text{ ml/sec}$, % removal at 600 sec = 65.52% and rising (SSVF), 75.16% and falling (ESVF).

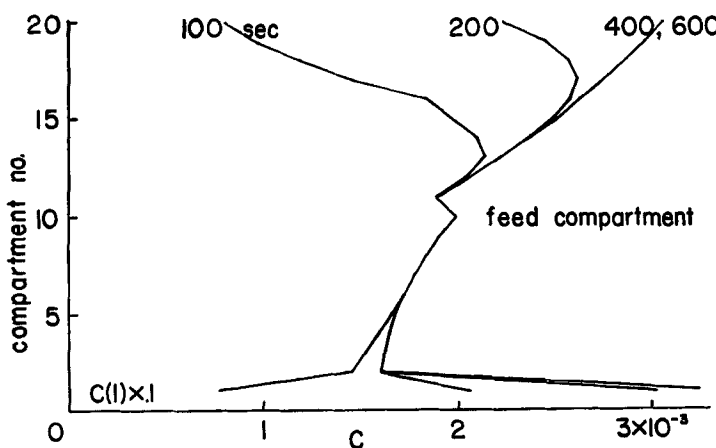


FIG. 14. Reactor-clarifier solids distribution. $Q_{\text{feed}} = 3000 \text{ ml/sec}$, % removal at 600 sec = 54.24% (SSVF), 55.50% (ESVF).

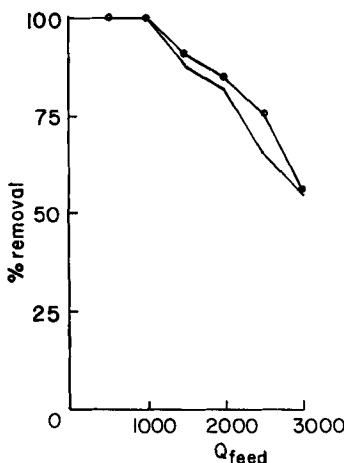


FIG. 15. Reactor-clarifier solids removals as functions of feed rate: (○) calculated from ESVF at 600 sec, (●) calculated from SSVF at 600 sec.

RESULTS, ANOTHER TYPE OF UPFLOW CLARIFIER

We last address ourselves to the design of the upflow clarifier shown in Fig. 3. The shape of the device is similar to the sludge blanket clarifier, but the feed is in the middle and sludge wasting takes place at the bottom, as with the reactor-clarifier. Figures 16, 17, and 18 exhibit the effect of decreasing solids volume fraction in the feed. The percent removals (SSVF) are given in Table 1.

The effect of feed rate on percent removal is indicated in Fig. 19. We note that the effect of overloading on this clarifier seems to fall midway between the effect of overloading on the other two designs, being more precipitous than that for the reactor-clarifier and less precipitous than that for the sludge blanket clarifier.

TABLE 1

Dependence of Percent Removal on Influent Solids Volume Fraction (ISVF)

ISVF	% removal (SSVF) (1200 sec)
0.01	98.27
0.05	74.86
0.10	63.95

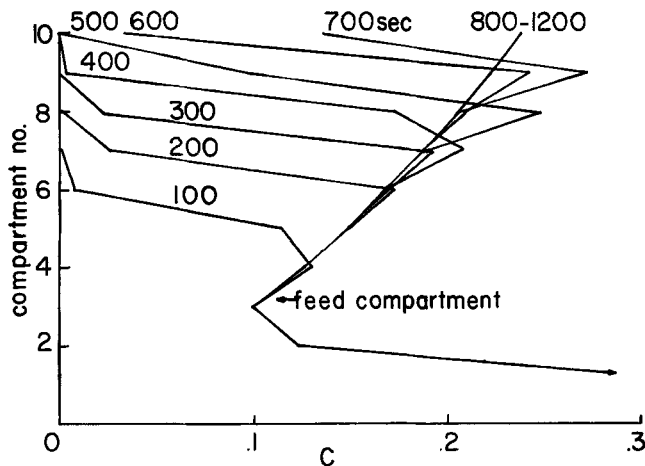


FIG. 16. Third upflow clarifier solids distribution. $r_u = 25$ cm, $r_e = 10$ cm, $l = 25$ cm, $L = 100$ cm, $\kappa = 0.1 \text{ sec}^{-1}$, $N = 5$, $I = 10$, ISVF = 0.10, $Q_{\text{feed}} = 700 \text{ ml/sec}$, $Q_{\text{waste}} = 83.3 \text{ ml/sec}$; other parameters as in Fig. 4. Percent removal at 1200 sec = 63.95% (SSVF), 63.96% (ESVF).

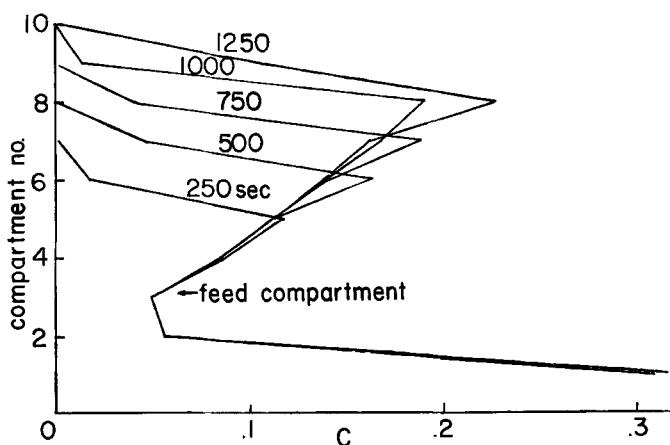


FIG. 17. Third upflow clarifier solids distribution. ISVF = 0.05; other parameters as in Fig. 16. Percent removal at 1200 sec = 74.86% (SSVF), 100.00% (ESVF).

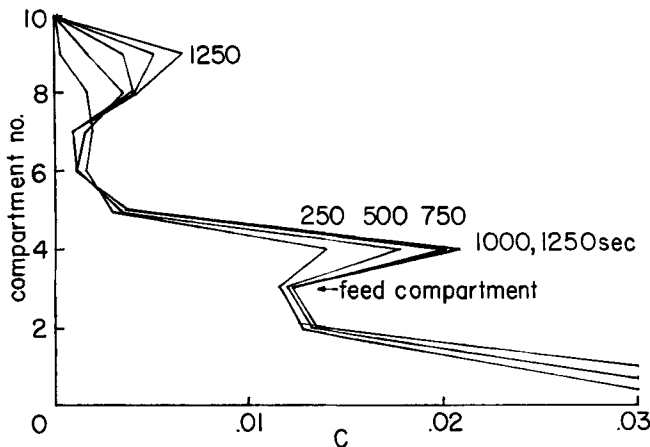


FIG. 18. Third upflow clarifier solids distribution. ISVF = 0.01; other parameters as in Fig. 16. Percent removal at 1200 sec = 98.27% (SSVF), 100.00% (ESVF).

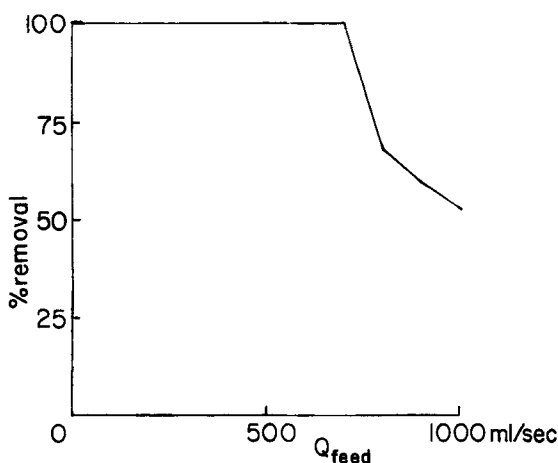


FIG. 19. Third upflow clarifier solids removals as functions of feed rate.

COMMENTS

In all three types of clarifiers the upper section of the clarifier (above the sludge wasting plane in the sludge blanket clarifier and above the feed plane in the other two) provides a buffer capacity to deal with short-term

heavy shock loadings. Monitoring the solids concentration somewhere near the bottom of the upper section of the clarifiers would evidently provide much better control of clarifier overflow quality (through feed rate adjustment) than monitoring solids in the clarifier overflow. The computer programs used permit one to estimate the effects of sudden shock overloads in solids concentration or feed rate of various magnitudes and durations. This information is needed to design the clarifier itself and to select the place for the monitoring equipment used to control overloading and maintain effluent quality.

The data presented here barely scratch the surface of what can be done with these clarifier simulators. The geometry of the clarifier (including the location of feed or sludge wasting planes), the effect of various feed rates and solids concentrations, the effects of particle density and size distribution, the effect of the rate of sludge wastage—all these can be economically simulated. In addition, with very minor modification, the programs could include the effects of a mixing tank and flow stabilizing device "up front" to determine whether these are optimal solutions to the problems of shock hydraulic and solids loadings.

These programs do not include terms for axial dispersion since we did not have any means for estimating axial dispersion constants; such terms could quite easily be added if desired. Also, the programs do not include a mechanism permitting the coalescence of particles of the same size. We believe that the energy dissipated in the liquid by the falling floc particles may provide such a mechanism through the small-scale turbulences which this creates; we are currently exploring this point.

Acknowledgments

This work was supported by a grant from the National Science Foundation. We are indebted to Professor Karl Schnelle and Ms. Elaine Graves for helpful discussions.

REFERENCES

1. K. J. Ives, *Proc. Inst. Civil Eng.*, 39, 243 (1968).
2. S.-C. Chang, "Computer Simulation of Flocculent Settling," Ph.D. Dissertation, Northwestern University, 1972.
3. J. H. Clarke, A. N. Clarke, and D. J. Wilson, *Sep. Sci. Technol.*, 13(9), 767 (1978).
4. D. J. Wilson, *Sep. Sci. Technol.*, 13(10), 881 (1978).

Received by editor April 3, 1978